The Function and Properties of the Iron−Sulfur Center in Spinach Ferredoxin:Thioredoxin Reductase: A New Biological Role for Iron−Sulfur Clusters†

Christopher R. Staples,‡ Emmanuel Ameyibor,‡ Weiguang Fu,‡ Laura Gardet-Salvi,§ Anne-Lise Stritt-Etter,§ Peter Schürmann,§ David B. Knaff,|| and Michael K. Johnson*,‡

Department of Chemistry and Center for Metalloenzyme Studies, University of Georgia, Athens, Georgia 30602, Laboratoire de Biochimie Végétale, Université de Neuchâtel, CH-2007 Neuchâtel, Switzerland, and Department of Chemistry and Biochemistry, Texas Tech University, Lubbock, Texas 79409

Received April 29, 1996⊗

ABSTRACT: Thioredoxin reduction in chloroplasts is catalyzed by a unique class of disulfide reductases which use a [2Fe-2S]$^{2+/+}$ ferredoxin as the electron donor and contain an Fe-S cluster as the sole prosthetic group in addition to the active-site disulfide. The nature, properties, and function of the Fe-S cluster in spinach ferredoxin:thioredoxin reductase (FTR) have been investigated by the combination of UV/visible absorption, variable-temperature magnetic circular dichroism (MCD), EPR, and resonance Raman (RR) spectroscopies. The results indicate the presence of an $S = 0$ [4Fe-4S]$^{2+}$ cluster with complete cysteinyl-*S* coordination that cannot be reduced at potentials down to −650 mV, but can be oxidized by ferricyanide to an $S = {}^1/_2$ [4Fe-4S]$^{3+}$ state ($g = 2.09, 2.04, 2.02$). The midpoint potential for the [4Fe-4S]$^{3+/2+}$ couple is estimated to be +420 mV (*versus* NHE). These results argue against a role for the cluster in mediating electron transport from ferredoxin ($E_m = -420$ mV) to the active-site disulfide ($E_m = -230$ mV, $n = 2$). An alternative role for the cluster in stabilizing the one-electron-reduced intermediate is suggested by parallel spectroscopic studies of a modified form of the enzyme in which one of the cysteines of the active-site dithiol has been alkylated with *N*-ethylmaleimide (NEM). NEM-modified FTR is paramagnetic as prepared and exhibits a slow relaxing, $S = {}^1/_2$ EPR signal, $g = 2.11, 2.00, 1.98$, that is observable without significant broadening up to 150 K. While the relaxation properties are characteristic of a radical species, MCD, RR, and absorption studies indicate at least partial cluster oxidation to the [4Fe-4S]$^{3+}$ state. Dye-mediated EPR redox titrations indicate a midpoint potential of −210 mV for the one-electron reduction to a diamagnetic state. By analogy with the properties of the ferricyanide-oxidized [4Fe-4S] cluster in *Azotobacter vinelandii* 7Fe ferredoxin [Hu, Z., Jollie, D., Burgess, B. K., Stephens, P. J., & Münck, E. (1994) *Biochemistry 33,* 14475−14485], the spectroscopic and redox properties of NEM-modified FTR are interpreted in terms of a [4Fe-4S]$^{2+}$ cluster covalently attached through a cluster sulfide to a cysteine-based thiyl radical formed on one of the active-site thiols. A mechanistic scheme for FTR is proposed with similarities to that established for the well-characterized NAD(P)H-dependent flavin-containing disulfide oxidoreductases, but involving sequential one-electron redox processes with the role of the [4Fe-4S]$^{2+}$ cluster being to stabilize the thiyl radical formed by the initial one-electron reduction of the active-site disulfide. The results indicate a new biological role for Fe-S clusters involving both the stabilization of a thiyl radical intermediate and cluster site-specific chemistry involving a bridging sulfide.

The chloroplast ferredoxin/thioredoxin system constitutes a mechanism whereby light regulates the activity of several carbon assimilation enzymes in oxygenic photosynthesis (Knaff & Hirasawa, 1991; Buchanan, 1992; Knaff, 1996). The light signal is transmitted in the form of electrons from the chlorophyll-containing thylakoid membranes *via* a [2Fe-2S] Fd, ferredoxin:thioredoxin reductase (FTR),[1] and thioredoxins which activate or deactivate target enzymes by reduction of regulatory disulfide bridges (see Scheme 1) (Buchanan et al., 1994). FTR catalyzes the key step in this important regulatory pathway, i.e., the two-electron reduction of the active-site disulfide in thioredoxin by sequential one-electron oxidations of the [2Fe-2S] ferredoxin (Fd). While FTR is known to contain an Fe-S cluster and an active-site disulfide (Droux et al., 1987), the properties and function of the Fe-S center have not been well-characterized.

Thus far FTR has been purified to homogeneity from spinach (Droux et al., 1987), corn (Droux et al., 1987),

† This work was supported by grants from the National Institutes of Health (R01-GM51962 to M.K.J.), the Schweizerischer Nationalfonds (31-28811.90 and 3100-37725.93 to P.S.), and the U.S. Department of Energy (DE-FG03-93ER20125 to D.B.K.), and by a Research Training Group Award to the Center for Metalloenzyme Studies (BIR-94-13236 to M.K.J.).

* Address correspondence to this author at the Department of Chemistry, University of Georgia, Athens, GA 30602. Telephone: 706-542-9378. FAX: 706-542-2353. E-mail: johnson@sunchem.chem.uga.edu.

‡ Department of Chemistry and Center for Metalloenzyme Studies, University of Georgia.

§ Laboratoire de Biochimie Végétale, Université de Neuchâtel.

|| Department of Chemistry and Biochemistry, Texas Tech University.

⊗ Abstract published in *Advance ACS Abstracts,* August 15, 1996.

[1] Abbreviations: Fd, ferredoxin; FTR, ferredoxin:thioredoxin reductase; T, thioredoxin; PSI, photosystem I; NEM, *N*-ethylmaleimide; NHE, normal hydrogen electrode; HiPIP, high-potential iron−sulfur protein; MCD, magnetic circular dichroism; RR, resonance Raman; DTT, dithiothreitol.

S0006-2960(96)01007-0 CCC: $12.00

Scheme 1: Thioredoxin-Dependent Regulation of Chloroplast Enzymes

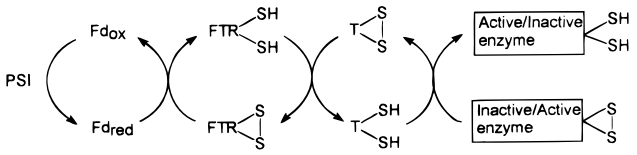

Nostoc muscorum (Droux et al., 1987), and *Chlamydomonas reinhardtii* (Huppe et al., 1990), and has been shown to be identical to the protein called ferralterin by previous workers (Lara et al., 1980; de la Torre et al., 1982). In each case, the enzyme was found to be a heterodimer with an apparent molecular mass of approximately 30 kDa. Subunit B (~13 kDa), which is also termed the catalytic subunit, contains the redox-active disulfide and the Fe-S cluster (Droux et al., 1987), and is common to all FTRs based on immunological cross-reactivity experiments (Droux et al., 1987; Huppe et al., 1990). Subunit A, which is also termed the variable subunit, differs in size and shows little or no immunological cross-reactivity among different species (Droux et al., 1987; Huppe et al., 1990).

Primary structures based on conventional protein sequence methods and/or deduced from the nucleotide sequence of cDNA clones have recently become available for the catalytic subunits of the FTRs from spinach (Chow et al., 1995; Falkenstein et al., 1994; Marc-Martin et al., 1993) and corn (Marc-Martin et al., 1993) and the variable subunits of the FTRs from spinach (Falkenstein et al., 1994; Iwadate et al., 1994) and the cyanobacterium *Anacystis nidulans* (Szekeres et al., 1991). The catalytic subunits of spinach and corn FTR (12.7 kDa) show 81% identity with seven conserved cysteines. Experiments involving modification of the eight cysteines in the catalytic subunit of spinach FTR with radioactively-labeled sulfhydryl-group blocking reagents, *N*-ethylmaleimide (NEM) and iodoacetate, have shown that the nonconserved Cys19 is not solvent-accessible, Cys27 is an accessible free thiol with no catalytic function, Cys54 and Cys84 constitute the active-site disulfide, and Cys52, Cys71, Cys73, and Cys82 are involved in ligating the Fe-S cluster (Chow et al., 1995). Hence, the redox-active disulfide is in close proximity to the Fe-S cluster. Moreover, in common with the majority of the NAD(P)H-dependent flavoprotein disulfide reductases (Thorpe & Williams, 1976; Arscott et al., 1981; Fox & Walsh, 1983), only one of the active site cysteines, Cys54, is accessible to sulfhydryl-group blocking reagents in reduced samples under nondenaturing conditions (Chow et al., 1995). The other active-site cysteine, Cys84, is labeled after reduction only under denaturing conditions, and appears to be protected from solvent and inaccessible to sulfhydryl reagents under native conditions (Chow et al., 1995). The variable subunit of spinach FTR has a molecular mass of 12.7 kDa and has one accessible free cysteine with no catalytic function, as judged by chemical modification experiments. Sequence analysis supports the view that this subunit has no catalytic function (Iwadate et al., 1994). Comparison with the variable subunit in the cyanobacterial FTR reveals 58% sequence similarity and the presence of a 30-residue N-terminal extension in the spinach protein which is likely to be responsible for the size variability and antigenic behavior of this subunit.

Purified FTRs contain approximately four non-heme iron atoms and acid-labile sulfides per molecule (Droux et al., 1987), and the UV−visible absorption and CD spectra (Droux et al., 1987; Schürmann & Gardet-Salvi, 1993; Hirasawa et al., 1988), coupled with the absence of an EPR signal , are most consistent with the presence of an $S = 0$ $[4Fe\text{-}4S]^{2+}$ cluster. However, EPR studies of spinach and *N. muscorum* FTRs showed no signals after reduction by dithionite, dithionite plus methyl viologen, or illuminated chloroplast membranes (de la Torre et al., 1982). This suggests that the cluster is not reducible to the paramagnetic state at potentials of −450 mV (*versus* NHE) and, therefore, that the cluster may not be effective in mediating electron transfer from chloroplast [2Fe-2S] Fds ($E_m = -310$ to -455 mV *versus* NHE) to the active-site disulfide. Rhombic EPR signals, $g = 2.10, 2.05, 2.00$ for spinach FTR and $g = 2.09, 2.04, 1.98$ for *N. muscorum* FTR, were reported at low temperatures (<30 K) for samples treated with ferricyanide (de la Torre et al., 1982). These were tentatively interpreted in terms of oxidation to an $S = {}^1/_2$ $[4Fe\text{-}4S]^{3+}$ state as found in oxidized high-potential iron−sulfur proteins (HiPIPs). However, this redox process is unlikely to be physiologically relevant in terms of mediating electron transfer since the potential was estimated to be + 410 mV *versus* NHE in *N. muscorum* FTR (de la Torre et al., 1982). More recently, direct electrochemical studies of spinach FTR reported a two-electron redox process with a midpoint potential of −230 mV that was attributed to the active-site disulfide, since it was not present in NEM-modified samples, and a one-electron process with a midpoint potential of +340 mV that was attributed to the $[4Fe\text{-}4S]^{3+/2+}$ couple (Salamon et al., 1995).

The objectives of this study were to characterize the electronic, magnetic, structural, and redox properties of the Fe-S center in spinach FTR with a view to elucidating its role in the catalytic mechanism. The approach involves using EPR, UV/visible absorption, variable-temperature magnetic circular dichroism (VTMCD), and resonance Raman (RR) spectroscopies to investigate the properties of the Fe-S cluster in native forms of the enzyme with the disulfide intact (native FTR) and reduced with dithiothreitol (DTT-treated FTR) and an inactive form of the enzyme in which one of the active-site cysteines, Cys54, has been modified with NEM (NEM-modified FTR). The results reveal the presence of a $[4Fe\text{-}4S]^{2+}$ cluster with complete cysteinyl ligation and suggest that the role of the cluster lies in stabilizing the one-electron-reduced intermediate rather than mediating electron transfer to the active-site disulfide. NEM-modified FTR appears to provide a stable analog of the one-electron-reduced intermediate, and the spectroscopic properties of this derivative are consistent with cluster coordination by one of the cysteines of the active-site dithiol. The mechanism that is proposed for FTR suggests a new biological role for Fe-S clusters.

MATERIALS AND METHODS

Sample Preparation and Handling. Purification of FTR from spinach (*Spinacea oleracea*) leaves was performed as previously described (Schürmann, 1995). The samples of spinach FTR used in this work had A_{410}/A_{278} ratios in the range 0.34−0.36 and were judged to be >90% pure by SDS−PAGE gel electrophoresis. Modification of one of the cysteines of the active site dithiol with NEM to give NEM-modified FTR was carried out as previously described (Chow et al., 1995; Schürmann & Gardet-Salvi, 1993). Sample

concentrations were based on $\epsilon_{410} = 17\,400\ M^{-1}\ cm^{-1}$ for native FTR (Droux et al., 1987) and $\epsilon_{410} = 19\,500\ M^{-1}\ cm^{-1}$ for NEM-modified FTR (Schürmann & Gardet-Salvi, 1993). Unless otherwise indicated, native FTR was in 20 mM phosphate buffer, pH 7.2, and NEM-modified FTR was in 20 mM triethanolamine hydrochloride buffer, pH 7.3. Samples were handled anaerobically in a Vacuum Atmospheres glovebox under argon (<1 ppm O_2).

Dithionite reduction was carried out under anaerobic conditions with a 15-fold stoichiometric excess of sodium dithionite in a 10−μL aliquot taken from a freshly prepared stock solution in 100 mM Tris-HCl buffer, pH 7.8. Deazaflavin-mediated photoreduction was carried out at 0 °C on anaerobic samples containing 10 mM sodium oxalate and 10 μM 5-deazaflavin, using an Oriel Corp. xenon arc lamp. Ferricyanide oxidation was performed aerobically by incubating samples with excess of potassium ferricyanide for 1−15 min at room temperature. For variable-temperature MCD studies, ferricyanide was removed by ultrafiltration using Centricon tubes with a YM10 membrane. The active-site disulfide in native FTR was reduced in DTT-treated FTR by incubation with a 50-fold stoichiometric excess of DTT for 1 h under anaerobic conditions (Droux et al., 1987).

EPR redox titrations were performed at ambient temperature (25−27 °C) in a Vacuum Atmospheres glovebox under argon (<1 ppm O_2), using 200 mM PIPES buffer, pH 7.0. Mediator dyes were added, each to a concentration of ca. 50 μM, in order to cover the desired range of redox potentials, i.e., methyl viologen, benzyl viologen, neutral red, safranin, phenosafranin, anthroquinone-1,5-disulfonate, indigodisulfonate, methylene blue, 1,2-naphthoquinone, duroquinone, and 1,2-naphthoquinone-4-sulfonate. Samples were first reduced by addition of excess sodium dithionite followed by oxidative titration with potassium ferricyanide. After equilibration at the desired potential, a 0.2-mL aliquot was transferred to a calibrated EPR tube and immediately frozen in liquid nitrogen. Potentials were measured with a platinum working electrode and a saturated calomel reference electrode and are reported relative to NHE.

Spectroscopic Measurements. UV/visible absorption spectra were recorded on a Shimadzu UV301PC spectrophotometer. Variable-temperature (1.5−300 K) and variable-field (0−6 T) MCD measurements were recorded on samples containing 50% (v/v) poly(ethylene glycol) using an Oxford Instruments SM3 or Spectromag 4000 split-coil superconducting magnet mated to a Jasco J-500C or J715 spectropolarimeter. The experimental protocols used in variable-temperature MCD studies for accurate sample temperature and magnetic field measurement, anaerobic sample handling, and assessment of residual strain in frozen samples have been described in detail elsewhere (Johnson, 1988; Thomson et al., 1993). The MCD intensities are expressed as $\Delta\epsilon$ ($\epsilon_{LCP} - \epsilon_{RCP}$) where ϵ_{LCP} and ϵ_{RCP} are the molar extinction coefficients for the absorption of left and right circularly polarized light, respectively. X-band (~9.5 GHz) EPR spectra were recorded on a Bruker ESP-300E EPR spectrometer equipped with an Oxford Instruments ESR-9 flow cryostat. Spin quantitations were carried out under nonsaturating conditions using 1 mM CuEDTA as the standard. Frozen solution EPR spectra were simulated with a modified version of the program QPOW developed by Prof. R. L. Belford and co-workers (Belford & Nilges, 1979; Nilges, 1979).

Raman spectra were recorded with an Instruments SA U1000 spectrometer fitted with a cooled RCA 31034 photomultiplier tube, using lines from Coherent Innova 10-W Ar^+ or Kr^+ lasers. Scattering was collected at 90° from the surface of a frozen 10−μL droplet of protein on the cold finger of an Air-Products Displex Model CSA-202E closed-cycle refrigerator. Band positions were calibrated using the excitation frequency and the principal bands of CCl_4 and are accurate to $\pm 1\ cm^{-1}$. The spectrum of the frozen buffer solution, normalized to the intensity of the ice-band at 230 cm^{-1}, and a linear ramp fluorescence background, has been subtracted from all the spectra shown in this work. Further details of the Raman spectrometer and the protocols used for obtaining low-temperature spectra of frozen anaerobic solutions are given elsewhere (Hamilton et al., 1989).

RESULTS

UV/visible absorption spectra for as-prepared and dithionite-reduced samples of native and NEM-modified spinach FTR are shown in Figure 1. The spectra of the as-prepared native and NEM-modified proteins are in excellent agreement with those reported previously (Schürmann & Gardet-Salvi, 1993). The absorption spectrum of native spinach FTR comprises a protein band at 278 nm, a shoulder at 315 nm, and broad shoulder centered at 410 nm. Such spectral characteristics are indicative of Fe-S proteins containing $[4Fe\text{-}4S]^{2+}$ clusters (Malkin, 1973). No significant change in the absorption spectrum was observed in samples that were treated aerobically with a 10-fold excess of ferricyanide followed by ultrafiltration to remove excess reagent, indicating little or no oxidation to the $[4Fe\text{-}4S]^{3+}$ state. Moreover, the pronounced shoulder at 410 nm is not lost on reduction by dithionite, indicating that the cluster is not reduced to the $[4Fe\text{-}4S]^{+}$ state. This result was also obtained for samples in which the active-site disulfide was reduced by preincubation with DTT (Droux et al., 1987), prior to dithionite treatment. More extensive changes in the absorption spectra accompany reduction of the NEM-modified spinach FTR. As prepared, the spectrum has resolved bands centered at 330 and 430 nm in addition to the protein band at 278 nm, and is characteristic of oxidized HiPIPs containing $[4Fe\text{-}4S]^{3+}$ clusters (Malkin, 1973). In accord with this interpretation, dithionite reduction results in a spectrum indistinguishable from that of native or dithionite-reduced FTR and consistent with one-electron reduction to the $[4Fe\text{-}4S]^{2+}$ state.

Resonance Raman in the Fe-S stretching region provides a much more discriminating assessment of cluster type and oxidation state (Spiro et al., 1988), and Figure 2 shows the spectra obtained using 457.9-nm excitation for native FTR, as prepared, and NEM-modified FTR, both as-prepared and dithionite-reduced. The enhancement pattern and frequencies for the Fe-S stretching modes in native FTR are characteristic of a $[4Fe\text{-}4S]^{2+}$ cluster with complete cysteinyl coordination (Spiro et al., 1988; Conover et al., 1990). Indeed, the spectra are very similar to those observed for $[4Fe\text{-}4S]^{2+}$ centers in structurally characterized synthetic model complexes such as $[Fe_4S_4(SCH_2Ph)_4]^{2-}$ and can be assigned by direct analogy under idealized T_d symmetry (Table 1) on the basis of the ^{34}S isotope shifts and normal mode calculations reported for this complex (Czernuszewicz et al., 1987). RR studies of $[4Fe\text{-}4S]^{2+}$ centers in Fds and HiPIPs indicate that reduction to the $[4Fe\text{-}4S]^{+}$ state is accompanied by a dramatic decrease

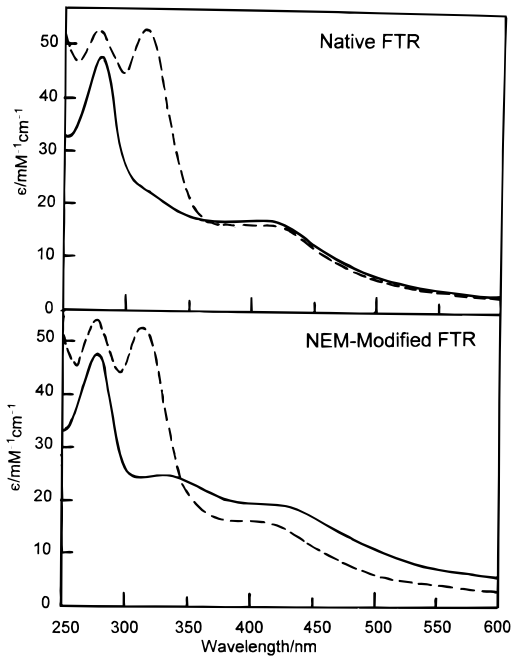

FIGURE 1: UV/visible absorption spectra of native (upper panel) and NEM-modified (lower panel) spinach FTR. In each case, the solid line represents the enzyme as-prepared, and the dashed line represents the enzyme anaerobically reduced with a 15-fold excess of sodium dithionite. The spectra were recorded in 1-mm cuvettes for samples that were 160 μM (native FTR) and 100 μM (NEM-modified FTR). The pronounced band at 314 nm in the dithionite-reduced samples originates from excess sodium dithionite.

in the resonance enhancement of Fe-S stretching modes using 457.9-nm excitation (Spiro et al., 1988), and that oxidation to the [4Fe-4S]$^{3+}$ state results in substantial changes in the relative intensities and frequencies of the Fe-S stretching modes (Backes et al., 1991; Moulis et al., 1988). However, no significant change in the RR spectrum of native FTR was observed after anaerobic reduction with DTT, dithionite, or DTT plus dithionite, or after aerobic oxidation with a 10-fold excess of ferricyanide, suggesting that the [4Fe-4S]$^{2+}$ cluster is largely inert to oxidation or reduction under these conditions.

Alkylation of one of the active-site cysteines in the NEM-modified sample has a pronounced effect on the RR spectrum; see Figure 2. The changes in the RR spectrum accompanying NEM modification can be accounted for in terms of increased cluster distortion from the idealized T_d symmetry, protein conformational changes in the vicinity of the cluster, oxidation to the [4Fe-4S]$^{3+}$ state, or a combination of two or all of these effects. For example, the enhancement of the E bridging mode and the splitting terminal T_2 mode could be interpreted in terms of increased distortion of the [4Fe-4S] core (Czernuszewicz et al., 1987). The RR spectra of biological [4Fe-4S] clusters are known to be sensitive to the cysteine Fe-S$_\gamma$−C$_\beta$−C$_\alpha$ dihedral angles, which determine the extent of coupling between the S$_\gamma$−C$_\beta$−C$_\alpha$ bending modes (expected near 310 cm^{-1}) and the terminal Fe-S stretching modes (Czernuszewicz et al., 1987; Backes et al., 1991). Greater coupling, resulting from one or more of the dihedral angles approaching 180°, might be expected to result in enhancement of the S$_\gamma$−C$_\beta$−C$_\alpha$ bending mode and a pronounced upshift for the A_1 terminal mode and splitting of the T_2 terminal, all of which are observed. The third possibility is that the changes arise from one-electron oxidation to the [4Fe-4S]$^{3+}$ state. Oxidation of [4Fe-4S]$^{3+/2+}$ clusters in HiPIPs is generally accompanied by upshifts of 1−5 cm^{-1} in the bridging Fe-S stretching modes and increased enhancement and upshifts of 9−29 cm^{-1} in the terminal Fe-S stretching modes (Backes et al., 1991; Moulis et al., 1988). While the frequency shifts for NEM-modified FTR are less than or in the low end of the ranges established for HiPIPs, the changes are generally consistent with oxidation of the cluster toward the [4Fe-4S]$^{3+}$ state. Support for the conclusion that cluster oxidation is responsible, at least in part, for the changes accompanying NEM modification comes from the observation that dithionite reduction of NEM-modified FTR restores the spectrum to a

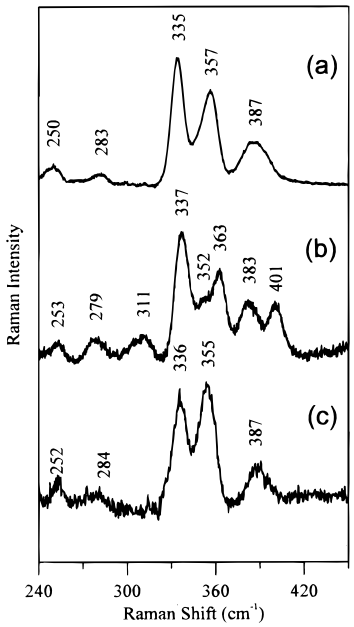

FIGURE 2: Resonance Raman spectra of native and NEM-modified spinach FTR. All spectra were recorded for samples frozen at 17 K using 457.9-nm laser excitation with 50 mW laser power at the sample. Each scan involved photon counting for 1 s at 0.2 cm^{-1} increments with 0.6 cm^{-1} spectral resolution. For all spectra, the vibrational modes originating from the frozen buffer solution have been subtracted after normalizing the intensities of the "ice-bands" at 230 cm^{-1}, and a linear ramp fluorescence background has been subtracted. (a) Native FTR (∼1 mM) as-prepared in 100 mM phosphate buffer, pH 7.6 (38 scans). NEM-modified FTR (∼0.6 mM) as-prepared in triethanolamine hydrochloride buffer, pH 7.3 (54 scans). (c) Dithionite-reduced NEM-modified FTR (∼0.5 mM) in triethanolamine hydrochloride buffer, pH 7.3, with a 15-fold excess of sodium dithionite (50 scans).

Table 1: Comparison of the Vibrational Frequencies (cm^{-1}) and Assignments for Native and NEM-Modified Spinach FTR and [Fe$_4$S$_4$(SCH$_2$Ph)$_4$]$^{2-}$ in Frozen Solutions

T_d assignment	spinach FTR[a] native	spinach FTR[a] NEM-modified	[Fe$_4$S$_4$(SCH$_2$Ph)$_4$]$^{2-}$ [b]
Mainly Terminal ν(Fe-S)			
A_1	387	401	389
T_2	357	363	360
		352	
Mainly Bridging ν(Fe-S)			
T_2	387	383	389
A_1	335	337	336
E or δ(S−C−C)		311	
T_1	283	279	273
T_2	250	253	244

[a] Frozen buffer solution at 17 K. [b] Frozen aqueous detergent medium consisting of 90/5/5 (vol %) H$_2$O/*N*,*N*-dimethylacetamide/Triton X-100 at 77 K (Czernuszewicz et al., 1987).

form closely resembling that of the $[4Fe\text{-}4S]^{2+}$ cluster in native FTR (see Figure 2). Hence, in addition to providing the most definitive spectroscopic data to date for the presence of a $[4Fe\text{-}4S]^{2+}$ in native FTR, the RR data support the absorption studies in finding that the cluster cannot be reduced by dithionite or DTT/dithionite and that NEM modification of one of the active-site cysteines results in a sample in which the cluster is formally in the $[4Fe\text{-}4S]^{3+}$ state.

EPR and VTMCD studies provide selective and complementary approaches for investigating the ground- and excited-state properties of Fe-S clusters with paramagnetic ground states. The EPR studies of native spinach FTR reported below are generally in agreement with those reported previously for ferralterin (de la Torre et al., 1982). However, the quantitative studies, over a wider temperature range that are reported herein, extend and necessitate significant changes in interpretation. As prepared, spinach FTR exhibited no EPR signals over the temperature range 4.2−100 K. Moreover, all attempts to reduce the cluster using dithionite, dithionite/DTT, dithionite/methyl viologen, and deazaflavin-mediated photoreduction failed to produce any evidence of a paramagnetic ($S = {}^1/_2$ or ${}^3/_2$) $[4Fe\text{-}4S]^{+}$ cluster as judged by both EPR and VTMCD studies. Hence, the midpoint potential for the $[4Fe\text{-}4S]^{2+/+}$ couple must be <-650 mV.

A fast-relaxing rhombic $S = {}^1/_2$ resonance, $g = 2.09$, 2.04, and 2.01, indicative of a $[4Fe\text{-}4S]^{3+}$ cluster and accounting for 0.30 ± 0.05 spin/[4Fe-4S] cluster, was observed at temperatures <30 K in samples of native spinach FTR oxidized with a 10-fold excess of ferricyanide (Figure 3). The high-field region of the resonance is obscured by overlap with a slower relaxing multiline signal centered at $g = 2.0$ that is most clearly observed at temperatures around 30 K. Studies as a function of varying power and temperature were required to delineate these two resonances (see Figure 3). The multiline resonance was present in varying amounts in different samples, with an intensity that increased with the excess of and/or length of incubation with ferricyanide, and was most clearly seen in samples treated with a 100-fold excess of ferricyanide (see Figure 3c). Quantitation under nonsaturating conditions indicated that it corresponds to ∼0.1 spin/molecule in such samples. It is attributed to a proton-split radical species of unknown origin. However, similar resonances have been reported on photochemical oxidation of tyrosyl residues in photosystem II (Warncke et al., 1994; Tommos et al., 1995), and assignment to an oxidized radical species associated with an aromatic residue, most likely a tyrosine, is our current working hypothesis. At higher temperatures around 70 K, the spectrum is dominated by a third resonance with $g = 2.11$, 1.99, 1.98 which quantifies to <0.05 spin/molecule. This resonance is identical to that observed in stoichiometric amounts in NEM-modified FTR, and its origin is discussed below.

Previous studies of spinach and *N. muscorum* ferralterin had reported resonances at $g = 2.10$, 2.05, 2.00, and $g = 2.09$, 2.04, 1.98, respectively, that were observed only below 30 K (de la Torre et al., 1982). The present studies indicate that the high-field *g*-value is misassigned due to overlap with the aromatic radical species. Both were tentatively attributed to $S = {}^1/_2$ $[4Fe\text{-}4S]^{3+}$ clusters on the basis of relaxation properties, $g_{av} > 2$, and midpoint potential. EPR redox titrations using samples poised with varying ferricyanide/ferrocyanide ratios indicated a midpoint potential of +410 mV for the $[4Fe\text{-}4S]^{3+/2+}$ couple in *N. muscorum* ferralterin. The observation that only ∼30% of the clusters in spinach FTR are oxidized with a 10-fold excess of ferricyanide, coupled with the observation that the EPR signal is lost on removal of excess ferricyanide by ultrafiltration, explains the absorption and RR results and suggests that the midpoint potential for the $[4Fe\text{-}4S]^{3+/2+}$ couple is ∼+420 mV. Dye-mediated EPR redox titrations of native spinach FTR to determine the midpoint potentials for this couple and the generation of the aromatic radical species are in progress. Since ferricyanide has an intense temperature-dependent UV/visible MCD spectrum, it was necessary to remove this reagent prior to MCD studies, and the resulting samples did not exhibit the characteristic temperature-dependent MCD bands of a $[4Fe\text{-}4S]^{3+}$ cluster. Nevertheless, the close correspondence in the properties of this EPR signal to those reported for other oxidized HiPIPs [typically $g = 2.12$, 2.04, 2.02 and observable only below 30 K (Antanaitis & Moss, 1976; Dunham et al., 1991)], coupled with the high redox potential [the $[4Fe\text{-}4S]^{3+/2+}$ couple in HiPIPs is in the range +50 to +450 mV (Meyer et al., 1983)], provides strong support for this interpretation.

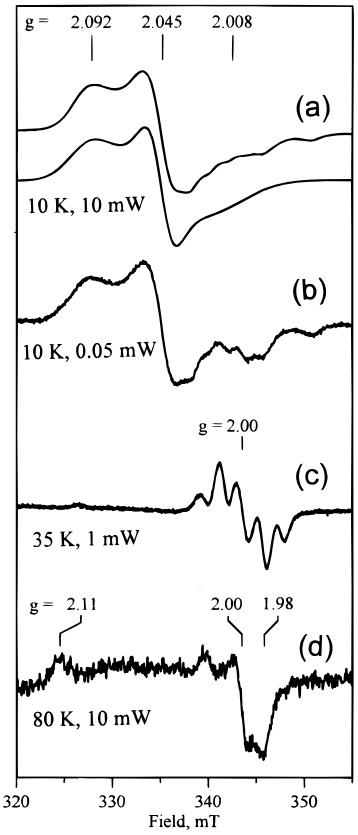

FIGURE 3: X-band EPR spectra of ferricyanide-oxidized native FTR. Native FTR (150 μM) was prepared in 100 mM phosphate buffer, pH 7.6, and oxidized aerobically by incubation for 2 min with a 10-fold excess of potassium ferricyanide for spectra (a), (b), and (d) and with a 100-fold excess of potassium ferricyanide for spectrum (c). EPR conditions: temperature and microwave power, as indicated; modulation amplitude, 0.63 mT; microwave frequency, 9.60 GHz.. The lower spectrum in (a) is a simulated powder EPR spectrum with $g = 2.092$, 2.045, and 2.008, with line widths of 7.7, 3.8, and 11.5 mT, respectively.

Very different EPR behavior was observed for NEM-modified FTR (see Figure 4). As-prepared NEM-modified FTR exhibits an intense axial $S = {}^1/_2$ resonance, $g = 2.11$,

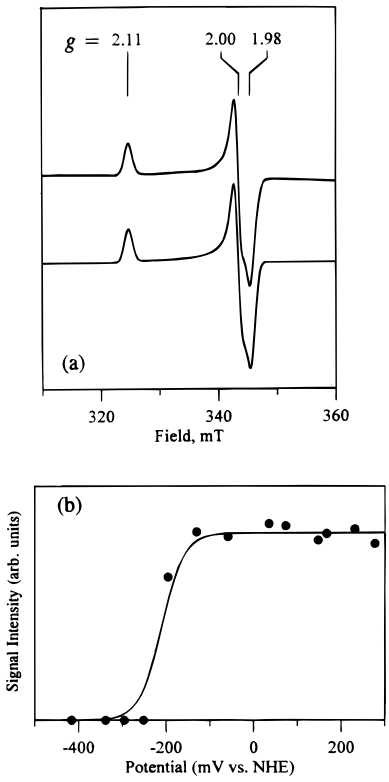

FIGURE 4: (a) X-band EPR spectrum of NEM-modified spinach FTR as-prepared. NEM-modified FTR (120 μM) was as-prepared in triethanolamine hydrochloride buffer, pH 7.3. EPR conditions: temperature, 50 K; microwave power, 1 mW; modulation amplitude, 0.63 mT; microwave frequency, 9.60 GHz. The lower spectrum is a simulated powder EPR spectrum with $g = 2.112$, 1.997, and 1.984, with line widths of 2.41, 1.90, and 2.38 mT, respectively. (b) EPR-monitored redox titration of NEM-modified spinach FTR. Data points correspond to the peak-to-trough intensity of the derivative-shaped feature centered at $g = 1.99$. The solid line is one-electron Nernst plot with $E_m = -210$ mV.

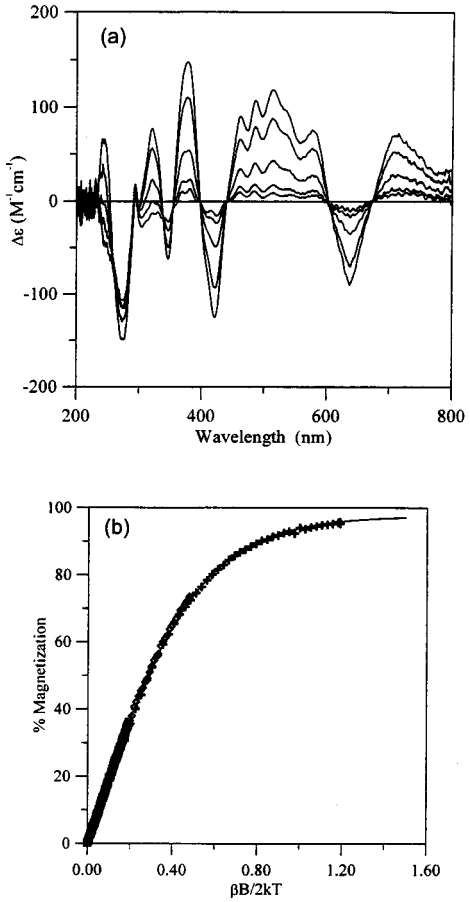

FIGURE 5: Variable-temperature MCD spectra and magnetization data for as-prepared NEM-modified spinach FTR. NEM-modified FTR (154 μM) in triethanolamine hydrochloride buffer, pH 7.3, with 50% (v/v) poly(ethylene glycol). (a) MCD spectra collected at 1.68, 4.22, 10.4, 25, and 43 K, with a magnetic field of 6 T. The intensity of all MCD bands (positive and negative) increases with decreasing temperature. (b) MCD magnetization data collected at 514 nm at 1.70 K (+), 4.22 K (◆), and 10.4 K (■) for magnetic fields in the range 0−6 T. The solid line is theoretical magnetization data for an $S = {}^1/_2$ ground state with $g_{\|} = 2.11$ and $g_{\perp} = 1.99$ (Thomson & Johnson, 1980; Bennett & Johnson, 1987).

2.00, 1.98, accounting for 1.00 ± 0.05 spin/molecule. The resonance is slow relaxing and observable without significant broadening up to at least 150 K. While such relaxation behavior is indicative of a radical species, the *g*-value anisotropy is more characteristic of an $S = {}^1/_2$ Fe-S cluster. The resonance was unperturbed by addition of a 10-fold excess of ferricyanide, but completely lost on dithionite reduction. No additional signals were observed over the temperature range 4.2−100 K in dithionite-reduced or ferricyanide-treated samples. Dye-mediated EPR redox titrations indicate that the loss of this resonance is associated with a one-electron redox process with a midpoint potential of −210 ± 30 mV (see Figure 4), well outside of the range reported for $[4Fe\text{-}4S]^{3+/2+}$ clusters in HiPIPs.

Variable-temperature MCD studies of NEM-modified FTR, as-prepared, revealed a complex pattern of temperature-dependent bands extending throughout the UV/visible/near-IR region (see Figure 5). MCD magnetization data confirm that the electronic transitions arise from an $S = {}^1/_2$ ground state and the data are well fit by theoretical plots constructed using EPR-determined *g*-values (Thomson & Johnson, 1980; Bennett & Johnson, 1987) (see Figure 5). Hence, the MCD bands arise from the same ground state responsible for the EPR signal. The MCD characteristics clearly indicate that the unpaired electron responsible for this resonance is associated with an Fe-S. However, comparison with the MCD spectra of known types of Fe-S clusters (Johnson et al., 1982; Onate et al., 1993; Fu et al., 1992; Richards et al., 1990; Marritt et al., 1995; Crouse et al., 1995; Finnegan et al., 1995) indicates a unique type of paramagnetic cluster with properties most closely resembling those of a $[4Fe\text{-}4S]^{3+}$ cluster. The pattern of bands is similar to that observed for oxidized HiPIPs in the 250−475 nm region (Johnson et al., 1981), but quite different in the lower energy region. Hence, while the absorption, RR, and MCD properties of NEM-modified FTR implicate the presence of some form of $[4Fe\text{-}4S]^{3+}$ cluster, the EPR and midpoint potential in particular indicate some unique properties compared to similar clusters in HiPIPs.

DISCUSSION

The detailed spectroscopic studies of spinach FTR reported herein leave no doubt that the Fd-dependent thioredoxin reductases from chloroplasts and cyanobacteria constitute a distinct family of disulfide reductases with properties and a catalytic mechanism very different from those of the extensive family of NAD(P)H-dependent disulfide oxidoreductases. The NAD(P)H-dependent disulfide oxidoreductase family of enzymes, which includes glutathione reductase, trypanothione reductase, lipoamide dehydrogenase, mercuric

ion reductase, NADH peroxidase, and thioredoxin reductase, all have homodimeric structures with NAD(P)H binding sites and contain one molecule of FAD and two redox-active cysteines that constitute the active-site disulfide (Williams, 1992; Waksman et al., 1994). On the basis of extensive structural data that are available for this family of disulfide reductases, it is clear that the tightly bound FAD mediates two-electron transfer from NAD(P)H to the disulfide and participates directly in the catalytic mechanism by binding one of the active-site thiols (the electron-transfer or flavin-interacting thiol), while the other (the interchange thiol) interacts with the substrate in a thiol−disulfide interchange reaction (Williams, 1992; Waksman et al., 1994).

The combination of absorption and RR studies of spinach FTR has provided unambiguous spectroscopic evidence that spinach FTR contains a cysteinyl-ligated [4Fe-4S]$^{2+}$ as the sole prosthetic group, in addition to the active-site disulfide. Moreover, the cluster must be in close spatial proximity to the active-site disulfide, since sulfhydryl alkylation experiments have shown that the active-site disulfide involves Cys54 and Cys84 while the cluster is ligated by Cys52, Cys71, Cys73, and Cys82, all within the catalytic subunit (Chow et al., 1995). The cluster is redox-inactive over the potential range −650 mV to at least +300 mV, but this work, and the previous EPR and electrochemical studies (de la Torre et al., 1982; Salamon et al., 1995), indicates that it can be oxidized to an $S = {}^1/_2$ [4Fe-4S]$^{3+}$ state at higher potentials. Prolonged exposure and/or large excesses of ferricyanide also result in an EPR signal that is tentatively attributed to a radical associated with an aromatic residue. However, such high-potential redox processes are unlikely to be physiologically relevant in light of the redox potentials of the electron donor ($E_m \sim -450$ mV) and the active site disulfide [$E_m \sim -230$ mV, $n = 2$ (Salamon et al., 1995)].

While the redox properties of native spinach FTR, deduced from the spectroscopic studies reported above, are in reasonable agreement with the direct electrochemistry results (Salamon et al., 1995), the same cannot be said for NEM-modified FTR. For native spinach FTR, a one-electron wave was observed at +340 ± 30 mV and attributed to the [4Fe-4S]$^{3+/2+}$ couple. In contrast, the EPR studies of *N. muscorum* FTR (de la Torre et al., 1982), and those of spinach FTR reported above, indicate that the midpoint potential for this couple is slightly above +400 mV. Clearly, caution must be exercised in attributing the observed wave in the cyclic voltammograms to a specific center, in light of the EPR evidence for oxidative generation of an aromatic radical species, and detailed EPR redox titrations of native FTR are in progress to resolve this issue. There is no reason to question the midpoint potentials for the disulfide/dithiol couples in spinach thioredoxins *f* and *m* (−210 ± 10 mV) and FTR (−230 ± 10 mV) determined by direct electrochemistry (Salamon et al., 1995), since they are in excellent agreement with the range of −200 to −300 mV reported for other thioredoxins (Moore et al., 1964; Berglund & Sjöberg, 1970; Porqué et al., 1970; Salamon et al., 1992; Rebeille & Hatch, 1986) and disulfide functional groups in general (Holmgren, 1981) at neutral pH. However, it is difficult to see how the cyclic voltammogram results for NEM-modified FTR, which reported only a one-electron wave with a midpoint potential of +380 ± 20 mV (Salamon et al., 1995), can be reconciled with the spectroscopic results reported here, which reveal a stoichiometric, cluster-related,

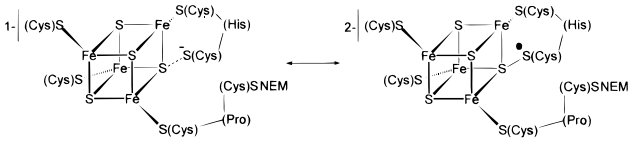

FIGURE 6: Proposed canonical structures for the Fe-S cluster in NEM-modified spinach FTR as-prepared.

one-electron redox process with a midpoint potential of −210 ± 30 mV. No evidence for an additional high-potential redox process was apparent in EPR redox titrations up to +400 mV or in samples treated with a 10-fold excess of ferricyanide. We are at a loss to explain this discrepancy, since we have obtained the same spectroscopic results for five distinct preparations of NEM-modified FTR.

The central problem that needs to be addressed in Fd-dependent thioredoxin reductases is how a one-electron donor, a [2Fe-2S]$^{2+/+}$ Fd ($E_m = -310$ to −450 mV), and an intrinsic [4Fe-4S]$^{2+}$ cluster ($E_m > +400$ mV and < -650 mV for the [4Fe-4S]$^{2+/+}$ and [4Fe-4S]$^{3+/2+}$ couples, respectively) can carry out a concerted two-electron reaction involving reductive cleavage of the active-site disulfide ($E_m = -230$ mV, $n = 2$) and subsequent reduction of the thioredoxin disulfide ($E_m = -210$ mV, $n = 2$). In light of the redox properties of the [4Fe-4S]$^{2+}$ center in spinach FTR, it seems extremely unlikely that this cluster is involved in mediating electron transfer from Fd to the active-site disulfide. As will be discussed below, the spectroscopic studies of the NEM-modified spinach FTR suggest an alternative role for the cluster in stabilizing the one-electron reduced intermediate and facilitate a rationale explanation of how this two-electron catalytic reaction can be broken down into sequential one-electron steps.

First it is important to emphasize that NEM modification involves photochemical reduction of the active-site disulfide in the presence of spinach Fd and heated thylakoid membranes and that only one of the active-site cysteines, Cys54, is alkylated under these conditions (Chow et al., 1995). The resulting sample is then repurified under aerobic conditions. By analogy with NAD(P)H-dependent disulfide reductases in which alkylation of one of the active-site cysteinates is prevented by direct interaction with the flavin isoalloxazine ring (Thorpe & Williams, 1976; Arscott et al., 1981; Fox & Walsh, 1983), the other active-site cysteine may be inaccessible to modification due to interaction with the [4Fe-4S] cluster. One-electron oxidation of the resulting species during aerobic purification would result in a species formally involving a [4Fe-4S]$^{3+}$ cluster interacting with the active-site thiol. In order to account for the spectroscopic properties of as-prepared NEM-modified FTR, a better description, or at least another canonical form, is likely to be a [4Fe-4S]$^{2+}$ covalently attached through a μ_3-S^{2-} to a cysteine-based thiyl radical (see Figure 6). While there is as yet no direct evidence for direct attachment of an active-site cysteinyl-*S* to a cluster-sulfide, the structures depicted in Figure 6 accommodate the anomalous spectroscopic and redox properties of NEM-modified FTR. For example, they account for absorption, RR, and MCD properties which suggest at least partial cluster oxidation toward an $S = {}^1/_2$ [4Fe-4S]$^{3+}$ state. In addition, they account for the anomalous relaxation properties and *g*-value anisotropy of the EPR signal which are best interpreted in terms of cluster-stabilized radical species. Finally, the one-electron redox potential ($E_m =$

Scheme 2: Proposed Mechanism for FTR

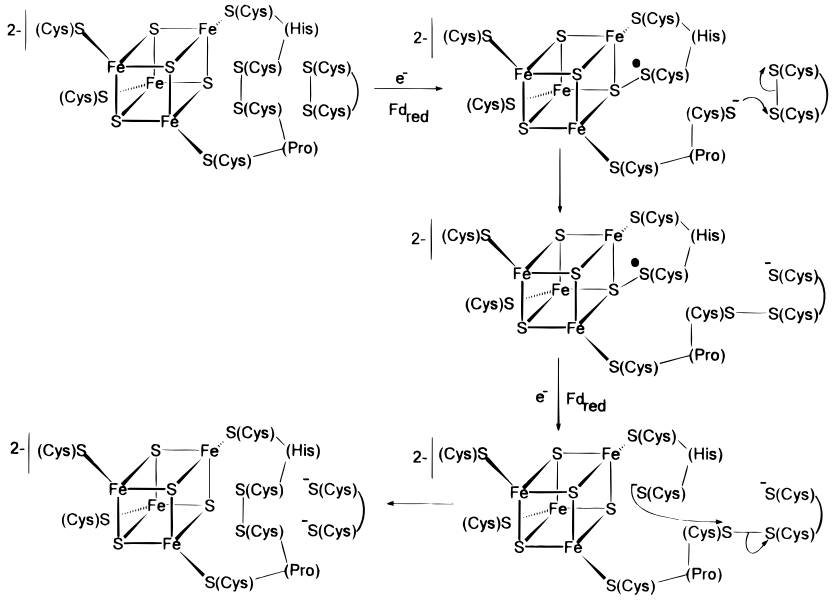

−210 mV) is close to that of the two-electron midpoint potential for reduction of the FTR and thioredoxin disulfides [E_m = −210 to −230 mV (Salamon et al., 1995)].

There is also a direct precedent for this type of chemistry in the 7Fe Fd from *Azotobacter vinelandii* (Morgan et al., 1984). Oxidation of the $[4Fe\text{-}4S]^{2+}$ cluster with ferricyanide results in an $S = {}^1/_2$ EPR signal, $g \sim 2.09$, 2.00, and 1.98, observable without significant broadening at temperatures above 77 K (Morgan et al., 1984), that is clearly very similar to that exhibited by NEM-modified FTR. Since this paramagnetic species appeared to exhibit negligible temperature-dependent MCD intensity, over and above that of the intense temperature-dependent bands originating from the $S = {}^1/_2$ $[3Fe\text{-}4S]^{+}$ cluster, it was tentatively identified as a cysteinyl disulfide radical, Cys-S-S$^{\bullet}$, arising from a three-electron oxidation of a $[Fe_4S_4(S\text{-}Cys)_4]^{2-}$ unit (Morgan et al., 1984). Subsequent mutagenesis experiments implicated a nonligating cysteine, Cys24, in this reaction (Iismaa et al., 1991), and X-ray crystallographic studies placed the S_γ of this residue 3.35 Å from a cluster sulfide (Stout, 1988). However, recent Mössbauer and EPR studies of ^{57}Fe-enriched protein have shown that the unpaired spin is coupled to cluster iron (Hu et al., 1994). This clearly ruled out the possibility of a magnetically isolated cysteinyl disulfide radical species, and raised the possibility "that the three-electron oxidation leads to the formation of a bond between cysteine 24 and one cluster sulfide" (Hu et al., 1994). Our spectroscopic and redox results for NEM-modified FTR show that the EPR resonance arises from a one-electron rather than a three-electron oxidation process and the structures proposed in Figure 6 are clearly applicable to the ferricyanide-oxidized form of the [4Fe-4S] cluster in *A. vinelandii* 7Fe Fd as well as NEM-modified FTR. While their interpretation has evolved as more data became available, the pioneering work of Stephens and Burgess on the anomalous properties of *A. vinelandii* 7Fe Fd (Morgan et al., 1984) has clearly set the stage for the emergence of a new role for biological Fe-S clusters in stabilizing radical intermediates of enzymatic reactions.

The question that remains is whether the NEM-modified form of spinach FTR is a nonfunctional curiosity or a candidate for a stabilized analog of the one-electron reduced enzymatic intermediate. A mechanistic scheme involving an equivalent one-electron-reduced intermediate and including the thiol−disulfide interchange reaction that has been established for NAD(P)H-dependent flavin-containing disulfide oxidoreductases (Williams, 1992) is presented in Scheme 2. The first electron from the reduced Fd is used to cleave the active-site disulfide, resulting in a cysteinate (interchange thiol) and a cluster-stabilized thiyl radical. The interchange thiol is then free to attack and cleave the substrate disulfide with the formation of a heterodisulfide. The resulting intermediate is the analog of NEM-modified FTR. Subsequent one-electron reduction of the cluster-stabilized thiyl radical species ($E_m \sim -210$ mV by analogy with NEM-modified FTR) results in the formation of a cysteinate on the cluster-interacting thiol. This species would be analogous to dithionite-reduced NEM-FTR. The catalytic cycle is then completed by the cluster-interacting thiol attacking and cleaving the heterodisulfide with re-formation of the active-site disulfide. At present, we have no direct evidence to suggest that NEM-modified FTR corresponds to the one-electron reduced intermediate in the enzymatic mechanism. Freeze−quench EPR experiments are planned to test this hypothesis. However, this species is unlikely to be an artifact of NEM modification, since it is observed to a small extent (<5%) in ferricyanide-oxidized samples of native spinach FTR. This can be rationalized by invoking the presence of a minor component of native FTR in which the active-site disulfide is reduced, provided cluster oxidation occurs more rapidly than dithiol oxidation.

The results presented here for FTR indicate a new biological role for Fe-S clusters involving both the stabilization of a radical intermediate and cluster site-specific chemistry involving a bridging sulfide. This begs the question of whether there is any evidence for similar functions in other Fe-S enzymes. Fe-S clusters are known to be present in at least three enzymes that function in radical mechanisms, i.e., anaerobic ribonucleotide reductase (Reichard, 1993), lysine 2,3-aminomutase (Frey & Reed, 1993), and biotin synthase (Sanyal et al., 1994). All three require *S*-adenosylmethionine, and Frey and Reed have proposed a

hypothetical mechanism for lysine 2,3-aminomutase whereby the cluster generates an adenosyl via site-specific chemistry at a cluster sulfide (Frey & Reed, 1993). However, there is as yet no direct evidence that the constituent Fe-S clusters are involved in stabilizing or generating radical intermediates in any of these enzymes. On the basis of spectroscopic and redox properties, there are clearly marked similarities in the properties of NEM-modified FTR with those of the H_2-activating Fe-S cluster in Fe-hydrogenases. This cluster contains 4−6 Fe atoms and is diamagnetic in the reduced state, but exhibits anomalous, slow-relaxing, $S = {}^1/_2$ EPR signals ($g \sim 2.10$, 2.04, 2.00 and $g \sim 2.07$, 2.01, 2.01 in CO- or O_2-treated samples, both observable without broadening at 70 K) on one-electron oxidation, $E_m = -360$ to -400 mV (Erbes et al., 1975; Adams, 1987, 1990; Kowal et al., 1989). Mössbauer and ^{57}Fe-ENDOR studies clearly demonstrate that the electron spin is coupled to cluster Fe, but the coupling constants are much smaller than those observed for conventional Fe-S clusters (Adams, 1990). Hence, an analogous cluster-bound thiyl radical species may also be responsible for the anomalous properties of the oxidized forms of this enzyme. A redox-active heterodisulfide involving a cysteine attached to a cluster sulfide is certainly an attractive possibility for the Fe-hydrogenase active site. Finally, the X-ray structure of the nitrogenase P-clusters indicates a disulfide linkage between cluster sulfides of the two bridged cubane clusters (Chan et al., 1993). If this disulfide is redox-active, it would provide an attractive candidate for a H_2-evolution site (Chan et al., 1993).

REFERENCES

Adams, M. W. W. (1987) *J. Biol. Chem. 262*, 15054−15061.

Adams, M. W. W. (1990) *Biochim. Biophys. Acta 1020*, 115−145.

Antanaitis, B. C., & Moss, T. H. (1976) *Biochim. Biophys. Acta 405*, 262−279.

Arscott, L. D., Thorpe, C., & Williams, C. H., Jr. (1981) *Biochemistry 20*, 1513−1520.

Backes, G., Mino, Y., Loehr, T. M., Meyer, T. E., Cusanovich, M. A., Sweeney, W. V., Adman, E. T., & Sanders-Loehr, J. (1991) *J. Am. Chem. Soc. 113*, 2055−2064.

Belford, R. L., & Nilges, M. J. (1979) *Computer Simulation of Powder Spectra*, EPR Symposium, 21st Rocky Mountain Conference, Denver, CO.

Bennett, D. E., & Johnson, M. K. (1987) *Biochim. Biophys. Acta 911*, 71−80.

Berglund, O., & Sjöberg, B.-M. (1970) *J. Biol. Chem. 245*, 6030−6035.

Buchanan, B. B. (1992) *Photosynth. Res. 33*, 147−162.

Buchanan, B. B., Schürmann, P., Decottignies, P., & Lozano, R. M. (1994) *Arch. Biochem. Biophys. 314*, 257−260.

Chan, M. K., Kim, J., & Rees, D. C. (1993) *Science 260*, 792−794.

Chow, L.-P., Iwadate, H., Yano, K., Kamo, M., Tsugita, A., Gardet-Salvi, L., Stritt-Etter, A.-L., & Schürmann, P. (1995) *Eur. J. Biochem. 231*, 149−156.

Conover, R. C., Kowal, A. T., Fu, W., Park, J.-B., Aono, S., Adams, M. W. W., & Johnson, M. K. (1990) *J. Biol. Chem. 265*, 8533−8541.

Crouse, B. R., Meyer, J., & Johnson, M. K. (1995) *J. Am. Chem. Soc. 117*, 9612−9613.

Czernuszewicz, R. S., Macor, K. A., Johnson, M. K., Gewirth, A., & Spiro, T. G. (1987) *J. Am. Chem. Soc. 109*, 7178−7187.

de la Torre, A., Lara, C., Yee, B. C., Malkin, R., & Buchanan, B. B. (1982) *Arch. Biochem. Biophys. 213*, 545−550.

Droux, M., Jacquot, J.-P., Miginac-Maslow, M., Gadal, P., Huet, J. C., Crawford, N. A., Yee, B. C., & Buchanan, B. B. (1987) *Arch. Biochem. Biophys. 252*, 426−439.

Dunham, W. R., Hagen, W. R., Fee, J. A., Sands, R. H., Dunbar, J. B., & Humblet, C. (1991) *Biochim. Biophys. Acta 1079*, 253−262.

Erbes, D. L., Burris, R. H., & Orme-Johnson, W. H. (1975) *Proc. Natl. Acad. Sci. U.S.A. 72*, 4795−4799.

Falkenstein, E., Vonschaewen, A., & Scheibe, R. (1994) *Biochim. Biophys. Acta 1185*, 252−254.

Finnegan, M. G., Conover, R. C., Park, J.-B., Zhou, Z. H., Adams, M. W. W., & Johnson, M. K. (1995) *Inorg. Chem. 34*, 5358−5369.

Fox, B., & Walsh, C. (1983) *Biochemistry 22*, 4082−4088.

Frey, P. A., & Reed, G. H. (1993) *Adv. Enzymol. Relat. Areas Mol. Biol. 66*, 1−39.

Fu, W., Drozdzewski, P. M., Davies, M. D., Sligar, S. G., & Johnson, M. K. (1992) *J. Biol. Chem. 267*, 15502−15510.

Hamilton, C. L., Scott, R. A., & Johnson, M. K. (1989) *J. Biol. Chem. 264*, 11605−11613.

Hirasawa, M., Droux, M., Gray, K. A., Moyer, J. M., Davis, D. J., Buchanan, B. B., & Knaff, D. B. (1988) *Biochim. Biophys. Acta 935*, 1−8.

Holmgren, A. (1981) *Trends Biochem. Sci. 6*, 26−29.

Hu, Z., Jollie, D., Burgess, B. K., Stephens, P. J., & Münck, E. (1994) *Biochemistry 33*, 14475−14485.

Huppe, H. C., de Lamotte-Guéry, F., Jacquot, J.-P., & Buchanan, B. B. (1990) *Planta 180*, 341−351.

Iismaa, S. E., Vazquez, A. E., Jensen, G. M., Stephens, P. J., Butt, J. N., Armstrong, F. A., & Burgess, B. K. (1991) *J. Biol. Chem. 266*, 21563−21571.

Iwadate, H., Yano, K., Kamo, M., Gardet-Salvi, L., Schürmann, P., & Tsugita, A. (1994) *Eur. J. Biochem. 223*, 465−471.

Johnson, M. K. (1988) in *Metal Clusters in Proteins* (Que, L., Jr., Ed.) ACS Symposium Series, Vol. 372, pp 326−342, American Chemical Society, Washington, DC.

Johnson, M. K., Thomson, A. J., Robinson, A. E., Rao, K. K., & Hall, D. O. (1981) *Biochim. Biophys. Acta 667*, 433−451.

Johnson, M. K., Robinson, A. E., & Thomson, A. J. (1982) in *Iron−Sulfur Proteins* (Spiro, T. G., Ed.) pp 367−406, Wiley-Interscience, New York.

Knaff, D. B. (1996) in *Oxygenic Photosynthesis: The Light Reactions* (Yocum, C. F., & Ort, D. R., Eds.) Kluwer Academic Publishers, Dordrecht (in press).

Knaff, D. B., & Hirasawa, M. (1991) *Biochim. Biophys. Acta 1056*, 93−125.

Kowal, A. T., Adams, M. W. W., & Johnson, M. K. (1989) *J. Biol. Chem. 264*, 4342−4348.

Lara, C., de la Torre, A., & Buchanan, B. B. (1980) *Biochem. Biophys. Res. Commun. 94*, 1337−1344.

Malkin, R. (1973) in *Iron−Sulfur Proteins* (Lovenberg, W., Ed.) pp 1−26, Academic Press, New York.

Marc-Martin, S., Spielmann, A., Stutz, E., & Schürmann, P. (1993) *Biochim. Biophys. Acta 1183*, 207−209.

Marritt, S. J., Farrar, J. A., Breton, J. L. J., Hagen, W. R., & Thomson, A. J. (1995) *Eur. J. Biochem. 232*, 501−505.

Meyer, T. E., Przysiecki, C. T., Watkins, J. A., Bhattacharyya, A., Simondsen, R. P., Cusanovich, M. A., & Tollin, G. (1983) *Proc. Natl. Acad. Sci. U.S.A. 80*, 6740−6744.

Moore, E. C., Reichard, P., & Thelander, L. (1964) *J. Biol. Chem. 239*, 3445−3452.

Morgan, T. V., Stephens, P. J., Devlin, F., Stout, C. D., Melis, K. A., & Burgess, B. K. (1984) *Proc. Natl. Acad. Sci. U.S.A. 81*, 1931−1935.

Moulis, J.-M., Lutz, M., Gaillard, J., & Noodleman, L. (1988) *Biochemistry 27*, 8712−8719.

Nilges, M. J. (1979) Ph.D. Dissertation, University of Illinois, Urbana, IL.

Onate, Y. A., Finnegan, M. G., Hales, B. J., & Johnson, M. K. (1993) *Biochim. Biophys. Acta 1164*, 113−123.

Porqué, P. G., Baldesten, A., & Reichard, P. (1970) *J. Biol. Chem. 245*, 2362−2370.

Rebeille, F., & Hatch, M. D. (1986) *Arch. Biochem. Biophys. 249*, 164−170.

Reichard, P. (1993) *J. Biol. Chem. 268*, 8383−8386.

Richards, A. J. M., Thomson, A. J., Holm, R. H., & Hagen, K. S. (1990) *Spectrochim. Acta 46A*, 987−993.

Salamon, Z., Gleason, F. K., & Tollin, G. (1992) *Arch. Biochem. Biophys. 299*, 193−198.

Salamon, Z., Tollin, G., Hirasawa, M., Gardet-Salvi, L., Stritt-Etter, A.-L., Knaff, D. B., & Schürmann, P. (1995) *Biochim. Biophys. Acta 1230*, 114−118.
Sanyal, I., Cohen, G., & Flint, D. H. (1994) *Biochemistry 33*, 3625−3631.
Schürmann, P. (1995) *Methods Enzymol. 252*, 274−283.
Schürmann, P., & Gardet-Salvi, L. (1993) *Chimia 47*, 245−246.
Spiro, T. G., Czernuszewicz, R. S., & Han, S. (1988) in *Biological Applications of Raman Spectroscopy* (Spiro, T. G., Ed.) Vol. 3: *Resonance Raman Spectra of Hemes and Metalloproteins*, pp 523−553, Wiley: New York.
Stout, C. D. (1988) *J. Biol. Chem. 263*, 9256−9260.
Szekeres, M., Droux, M., & Buchanan, B. B. (1991) *J. Bacteriol. 173*, 1821−1823.
Thomson, A. J., & Johnson, M. K. (1980) *Biochem. J. 191*, 411−420.
Thomson, A. J., Cheeseman, M. R., & George, S. J. (1993) *Methods Enzymol. 226*, 199−232.
Thorpe, C., & Williams, C. H., Jr. (1976) *J. Biol. Chem. 251*, 3553−3557.
Tommos, C., Tang, X.-S., Warncke, K., Hoganson, C. W., Styring, S., McCracken, J., Diner, B. A., & Babcock, G. T. (1995) *J. Am. Chem. Soc. 117*, 10325−10335.
Waksman, G., Krishna, T. S. R., Williams, C. H., Jr., & Kuriyan, J. (1994) *J. Mol. Biol. 263*, 800−816.
Warncke, K., Babcock, G. T., & McCracken, J. (1994) *J. Am. Chem. Soc. 116*, 7332−7340.
Williams, C. R., Jr. (1992) in *Chemistry and Biochemistry of Flavoenzymes* (Müller, F., Ed.) Vol. III, pp 121−211, CRC Press, Boca Raton, FL.

BI961007P